scientific reports

Check for updates

OPEN

The Cenomanian/Turonian boundary in light of new developments in terrestrial palynology

Francesca Galasso[1]✉, Ulrich Heimhofer[2] & Elke Schneebeli-Hermann[1]

The Cenomanian/Turonian boundary interval is associated with an oceanic anoxic event (OAE 2, 94.0 Ma) during one of the warmest episodes in the Mesozoic. To date, plant responses to these climatic conditions are known only from the northern mid-latitudinal succession in Cassis, France. There, conifer-dominated and angiosperm-dominated vegetation types alternate. However, whether the exceptional environmental conditions had an impact on plant reproduction is unknown to date. We applied a new environmental proxy based on spore and pollen teratology on palynological samples from the Cassis succession, to explore if this phenomenon also occurs across the OAE 2. The observed frequencies of<1% malformed spores and pollen grains suggest that plant reproduction was not affected during the Cenomanian/Turonian boundary interval. While the effects of continental Large Igneous Province(s) on plant reproduction have shown to produce abnormal spore or pollen morphologies as evidence for severe environmental pollution, by contrast the effects of oceanic LIP(s) seems to be inconsequential.

Teratology is the science of malformation that occurs during the development of an organism. Spores and pollen are also known to show teratomorph morphologies, sometimes in frequencies exceeding the background values of plants grown under present-day natural conditions[1].

In paleopalynology, teratomorphic spores and pollen have been successfully employed as a proxy for increased environmental disturbance. The occurrence of increased malformation in sporomorphs represents one of the more exotic proofs of stress response in biotas during the Devonian/Carboniferous boundary (DCB,[2]), the Permian/Triassic boundary (PTB,[3–5]), the Smithian/Spathian boundary (SSB,[6]), the Triassic/Jurassic boundary (TJB,[7–10]) and the Toarcian Oceanic Anoxic Event (T-OAE,[11,12]). Although much progress has been made in studying the vegetation response to environmental perturbations throughout the Mesozoic, the Cretaceous, particularly the Cenomanian/Turonian boundary, is still poorly studied and understood.

The early Late Cretaceous is one of those intervals in the Phanerozoic, which are characterised by "greenhouse" climate conditions[13]. During this period, ecosystems have experienced severe paleoenvironmental stress related to the warmest climate of the previous 150 Ma[14]. Especially the Cenomanian/Turonian transition (about 93.9 Ma,[15]) is characterised by profound paleoenvironmental changes on a global scale. The boundary interval is marked by an extinction event and turnover in planktonic foraminifera and radiolarians[16–21], by an increase in sea level[22–26], and by widespread dysoxic to anoxic conditions known as the Oceanic Anoxic Event 2 (OAE 2). The widespread anoxia-euxinia resulted in the depletion of isotopically light ^{12}C in seawater due to increased organic matter burial, globally expressed by a positive carbonate excursion (CIE) in both marine and terrestrial organic and inorganic carbon (e.g.[27–31]). In addition to a major transgression, the time interval encompassing OAE 2 was dominated by oceanic anoxia and acidification and a biocalcification crisis where calcareous nannoplankton experienced anomalous paleoceanographic and paleoclimatic conditions that induced extinctions as well as originations (e.g.[14,20,32,33]). However, recently the decline of calcareous microfossils has been questioned by the observation of "ghost" nannofossils[34]. Along with the widespread anoxia, the onset of OAE 2 was accompanied by a rise in sea surface temperature (SST), known as the "Cretaceous thermal maximum", which most likely occurred as abrupt warming associated with an increase in atmospheric pCO_2 (e.g.[24,35–40]). These warm conditions and high pCO_2 during the OAE 2 were interrupted by a transient period of climate instability (with

[1]Paleontological Institute and Museum, University of Zurich, Karl-Schmid-Strasse 4, 8006 Zurich, Switzerland. [2]Institute of Geology, Leibniz University Hannover, Callinstrasse 30, 30167 Hannover, Germany. ✉email: francesca.galasso@pim.uzh.ch

multiple short SST drops and rises in the range of 2.5 − 11 °C), re-oxygenation of the oceans, and a shift in the vegetation community, named the Plenus Cold Event (PCE) (e.g.[29,35,37,38,40–44]). The environmental changes and biotic responses during the OAE 2 have been tentatively linked to the emplacement of widespread submarine basaltic plateaus of large igneous provinces (LIPs; the Caribbean and High Arctic LIPs)[45–56]. LIPs released huge volumes of CO_2 and introduced high concentrations of biolimiting metals into the ocean and atmosphere[46] that possibly resulted in ocean fertilisation and/or poisoning by toxic metals[20,33] affecting both terrestrial and marine communities.

The sedimentary succession at Cassis (southeast France) has been well-calibrated by ammonoid[57], planktonic foraminifera, and nannofossil biostratigraphy[58], and $\delta^{13}C_{org}$ chemostratigraphy[38]. The palynological data of the Cassis section provides the first complete assessment of plant responses during the OAE 2[38]. Palynological studies in this region have identified two alternate vegetation types. (1) During the Cretaceous thermal maximum, the vegetation was characterised by a dominance of conifers growing in mesic habitats with moderate availability of moisture[38], although the high temperatures might have played a critical stress factor on the vegetation and plant development, even by partially slowing photosynthesis with temperature exceeding 35 − 40 °C[13]. (2) During the PCE, cooler climate and less humid conditions favoured open, savanna-type vegetation dominated by angiosperms[38]. However, the environmental proxy based on spore and pollen teratology has not been applied so far.

According to Green et al.[59], the major Phanerozoic extinction events may be triggered by comparable mechanisms related to continental flood basalt emplacement. In light of the repeated observations of malformed sporomorphs during times of major biotic crises, in this contribution we evaluate whether teratomorphies occur during the Cenomanian/Turonian boundary interval and which potential causes ascribed to this phenomenon are reflected in the geological record.

Geological setting

The Cassis sedimentary succession is exposed along the French Mediterranean coastline, stretching from Pointe des Lombards in the town of Cassis towards the southeast to the foot cliff of Cap Canaille (Fig. 1).

The section is 235 m thick and encompasses the Grès de l'Anse Sainte Magdeleine Fm. and the Calcaires du Corton Fm. (lower upper Cenomanian), and the Marls de l'Anse de Arène Fm. (upper Cenomanian to lower Turonian). The base of the studied succession is located 500 m southeast of the Cassis marina at Pointe de Lombards (43°12′ 34.0″ N 5°32′ 23.0″ E) and is characterised by a monotonous lithology of clays and marls, interbedded with turbiditic sandstones at the top of the Grès de l'Anse Sainte Magdeleine Fm. (0–19.7 m) (Fig. 2), followed by a 10-meter-long gap in the outcrop. The overlaying Calcaires du Corton Fm. (33.4–46.1 m) is characterised by calcareous marls and limestones with intense slumping structures of the Calcaires du Corton Fm., subsequently interrupted by a second gap. The upper part of the section (55.8–236.0 m) is represented by continuous grey marls deposits and a series of nodular limestone layers (labelled a-f in Fig. 2) corresponding to the Marls de l'Anse de Arène Fm. For further in-depth information on the Cassis section's sedimentology, chemo- and biostratigraphy, see[38].

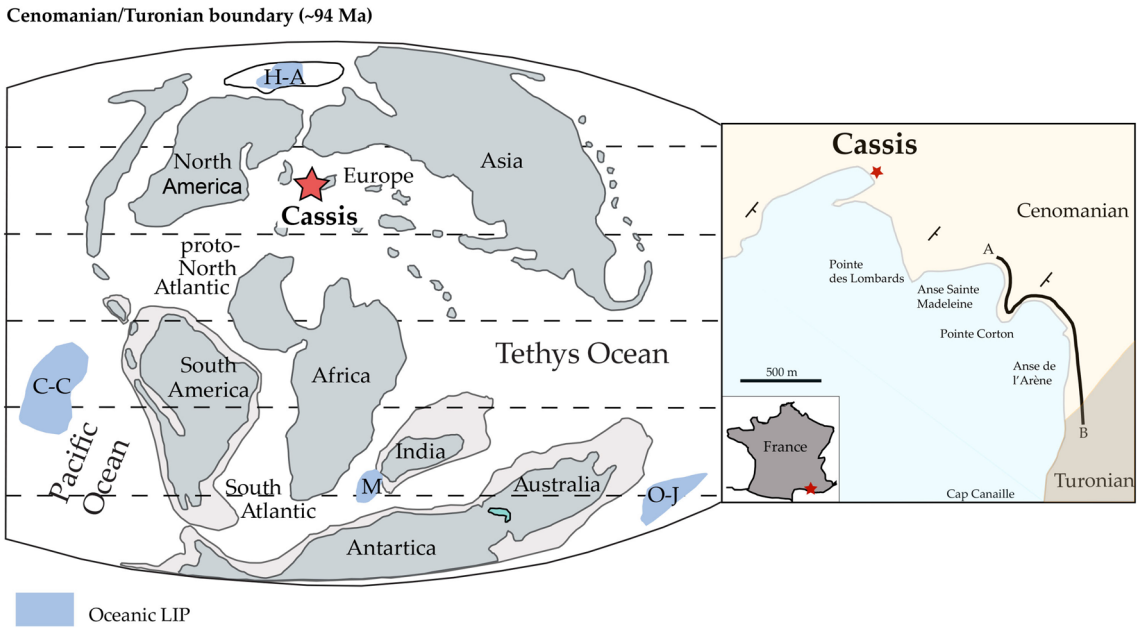

Figure 1. Simplified Late Cretaceous paleogeographical map, location map and the studied stratigraphic section (**A**, **B**). Figures modified after[57,60], respectively.

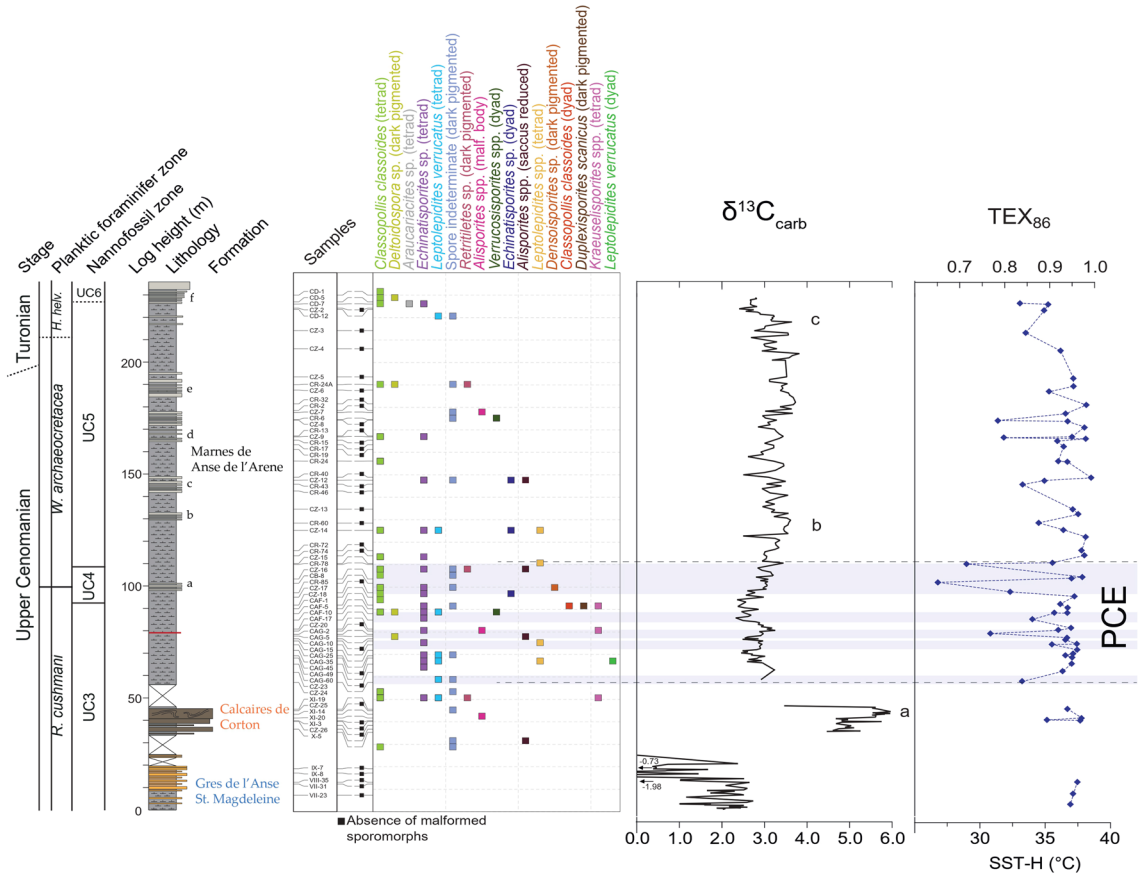

Figure 2. Stratigraphical distribution of malformed sporomorphs in the Cassis section. Presence/absence data of abnormal morphological variation in sporomorphs. Each cross represents a minimum of two occurrences of the respective sporomorph. Lithological log, biostratigraphy, $\delta^{13}C_{carb}$, $\delta^{13}C_{org}$, TEX_{86}-derived sea-surface temperatures (SSTs) adapted from[38]. PCE = Plenus Cold Event. Blue horizontal bands represent individual SST cooling episodes during the PCE.

Results

The preservation of palynomorphs in the Cassis section varies markedly, ranging from moderate to good. The rich and diverse spore-pollen assemblage of the Cassis section is dominated by inaperturate and bisaccate gymnosperm pollen produced by Araucariaceae and Cupressaceae-type plants (*Araucariacites* spp., *Inaperturopollenites* spp.), Cheirolepidiaceae (*Classopollis* spp.) and by angiosperm pollen of the Normapolles-type-group, including *Atlantopollis* and *Complexiopollis*. On the other hand pteridophytes produced by a diverse assemblage of ground ferns and fern allies were present in a negligible amount. The first shift in the floral association occurred with the inception of the PCE where a dominance of Normapolles-type pollen (e.g. *Atlantopollis microreticulatus*) coincides with the decline of conifer pollen contents (e.g. *Inaperturopollenites* spp., see Fig. 3 (AZ III) in[38]). With stratigraphic height, the spore-pollen assemblage shows a major change in frequency distribution patterns including a pronounced increase in *Inaperturopollenites* spp. followed by a decline in certain species of *Atlantopollis* (pronounced in *Atlantopollis microreticulatus*), see Fig. 3 (AZ VI) in[38].).

After a thorough screening of the palynological slides of the Cassis section, almost no malformed sporomorphs were found, except for the seldom occurrences of spore/pollen tetrads and dyads (Fig. 3). Spore dyads, including *Densoisporites* spp. and *Leptolepidites verrucatus*, were found in a single arrangement—two grains close/attached one to the other. Furthermore, spore tetrads of the taxa *Echinatisporis echinoides*, *Leptolepidites* spp., *Kraeuselisporites* spp., and *Retitriletes* spp., as well as pollen tetrads such as *Araucariacites* sp., and *Classopollis classoides* were found as welded grains or as grains close/attached to one another. Despite changes in plant community, such as the radiation of angiosperms and the proliferation of cold and less humid savanna-type vegetation[38] coinciding with the PCE, we acknowledge the presence of teratological lycophyte spore tetrads, i.e. *Echinatisporis* spp. and *Leptolepidites verrucatus*. Furthermore, *Leptolepidites* spp. was also recorded in a single occurrence as a spore dyad in sample CAG-35. Lycophytes, as well as ferns, are best represented in environments with high humidity and moderate temperatures in tropical and subtropical forests[61]. However, many species are also morpho-ecophysiologically adapted to low water availability and extreme temperatures[62]. The variety of habitats in which ferns and lycophytes can occur reflect their diverse strategies in response to environmental pressures[63].

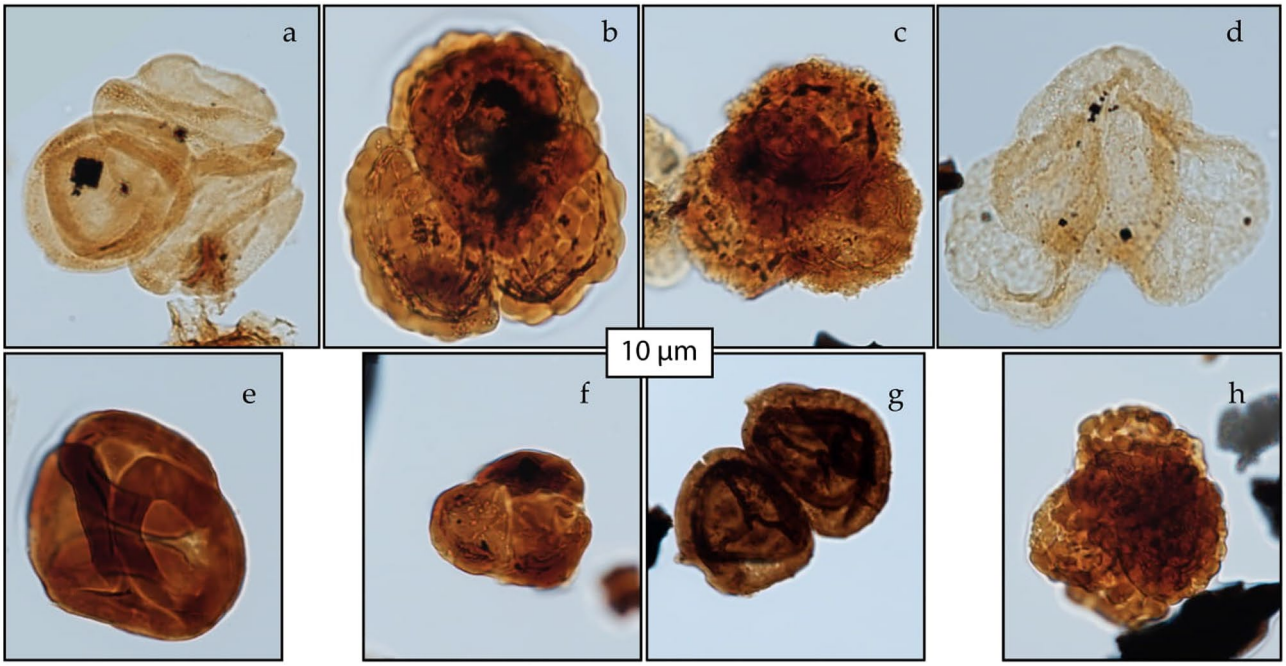

Figure 3. Selected spores and pollen from the OAE 2 of Cassis (southeast France). The sample number is followed by England Finder coordinates.**(a), (f)= *Classopollis classoides* (tetrad)**, sample CAF 10, V51/4; CB 8, O34/1; **(b), (h)= *Leptolepitides* sp. (tetrad)**, sample CAG 35, O30; XI-M-19, K36/1; **(c)= *Kraeuselisporites* sp. (tetrad)** sample CAF 5, Y35; **(d)= *Alisporites* sp. (expanded central body and folded left saccus)**, sample CAG 2, X50; **(e)= *Classopollis classoides* (welded grains tetrad)**, sample XI-M-19, O41/3; **(g)= *Densoisporites* sp. (dyad)**, sample CZ 17, U43.

Classopollis classoides in the Cassis section had somewhat comparable sizes to dispersed *Classopollis*, which ruled out polyploidy[11,12,64]. It is known to frequently occur in tetrads[65] in low-energy shelf environments or oceanic sediments that were deposited far from land[66,67]. As a result, the presence of *Classopollis* tetrads is not necessarily a sign of environmental disturbance. Although the genus is commonly associated with semiarid to arid climates (e.g.[68]), it has also been described from coastal environments or areas subject to repeated volcanic ash fall, indicating its ability to adapt to dry, saline, or even disturbed habitats (e.g.[69,70]). Besides, the presence of *Classopollis classoides* tetrads during the PCE contrast with the disappearance or sporadic occurrence of the taxon described from the nearby Pont d'Issole section (Unit Th2)[71].

Along with changes in size and form, we also noticed sporomorph color variations in the Cassis section. While *Leptolepidites* spp. and other spores with thick and ornamented sporomorph wall were ignored, spores with medium and smooth exine, such *Deltoidospora* spp., had occasionally a darker color. This peculiar characteristic, though, could be the result of a taphonomic artefact rather than environmental stress; therefore, further studies are needed to validate this external trait. The few occurrences of spore dyads and tetrads were less than 1% on average and, therefore, below the baseline frequency of 3-5% above which environmental influence on spore and pollen morphology can be assumed[1,8,12,72]. They reflect the natural variation of spore and pollen morphology (e.g.[73,74]). However, the stratigraphic frequency distribution of sporomorph malformations and tetrads has revealed a buildup of these malformations coinciding with the PCE (Fig. 2). As opposed to sporomorphs, a complete lack of malformation was found in another palynomorph group- the angiosperms. While polyploidy is an unusual phenomenon among extant gymnosperm, it is common in flowering plants[64,75]. Angiosperm might have been unaffected by the harsh environmental conditions experienced at the OAE 2 by applying a successful strategy as hybridization or polyploidizations (whole-genome duplications).

Discussion

The Earth's climate has changed dynamically over geological time, oscillating between two primary states: the "Icehouse" state and the "Greenhouse" state. The climate in each of the states varied significantly, and additional driving forces modified climatic conditions, either leading to cooler or warmer climates. Large igneous provinces (LIPs) are enormous crustal emplacements (millions of km^3) of predominantly mafic extrusive and intrusive rocks originating via processes other than "normal" seafloor spreading, e.g. continental flood basalts (or traps), volcanic passive margins, oceanic plateaus, and seamount groups[76]. The emplacement of LIPs can be related to hyperthermal events in Earth history. For example, the Siberian Traps are associated with the Permian/Triassic boundary, the Central Atlantic Magmatic Province with the End Triassic, the Karoo-Ferrar with the Toarcian OAE and the Caribbean and the High Arctic with the Cenomanian/Turonian boundary, among others. Comparing various LIPs and associated environmental and biotic responses, e.g. the Permian/Triassic boundary (PTB, 252 Ma), the Smithian/Spathian boundary (SSB 249.2 Ma), the Triassic/Jurassic boundary (TJB, 201.51 Ma), the early Toarcian oceanic anoxic event (T-OAE, 183 Ma), and the Cenomanian oceanic anoxic event (OAE

2, 94 Ma) the severity of their effect on climate and biota differs. The PTB, SSB, TJB, and T-OAE are associated with continental LIPs. Proxy evidence for volcanism in stratigraphic strata points to a strong temporal correlation between LIP volcanism and climate warming, reflecting the beginning of environmental change[77–83]. Continental LIPs eruptions caused significant changes in temperature, habitat, and biota in both marine and continental settings. The dramatic $\delta^{13}C$ anomalies were attributed to the catastrophic release of highly volatile methane hydrates originating from intruded volatile-rich sediments such as organic-rich shales, coals, and evaporates by LIP magmas[84–86], leading to a runaway greenhouse. This is, in turn, assumed to have been triggered by the massive release of volcanic CO_2. Depending on the individual components of volcanic gas release, the effects on the atmosphere and continental environments involved global warming, an increase in wildfires and droughts, intensified continental weathering and terrigenous input, acid rain, ozone layer destruction, metals poisoning, and cooling, which caused profound changes on land ([82,87]).These changes include for instance, a shift in plant-community dominance structure from pollen-dominated to a spore-dominated ecosystems (i.e. spore "spike") (e.g.[88–94]), and the occurrence of malformed pollen and spores beyond background values (e.g.[2,5,7–12]). In both cases, the harmful effects of LIPs, such as halocarbons, SO_2, and phytotoxicity, were ascribed as the potential causes[7,8,95]. By contrast, the OAE 2 resulted from submarine LIP emplacement on oceanic crust.The OAE 2 was associated with two LIPs, including the Caribbean-Columbian Plateau and the High Arctic LIP[45–56]. The effects of submarine LIPs eruption on the environment included widespread anoxia, the large-scale burial of organic matter, toxic metals, global warming or cooling and the partial demise of carbonate platforms. Given that the volcanism occurred predominantly below the sea surface, the effect of released gases was buffered by seawater[82]. Therefore, the impact on the deep-sea biota was much more severe than on shallow marine and terrestrial biota. Compared to other major biotic crises in the Earth's history, the OAE 2 has shown an extremely low abundance of malformed spores and pollen. This suggested that likely variations between different types of LIPs in terms of emplacement and eruptive style (e.g. submarine vs subaerial volcanism and additional thermogenic emissions) caused different responses of global vegetation. In summary, the Cenomanian/Turonian boundary succession in Cassis revealed only a few malformed spores and pollen grains. The extremely low abundance of teratomorphs found across the OAE 2 indicates only minor stress-related effects on land plant reproduction. Perhaps the mode of LIP emplacement and the associated volatiles coinciding with the Cenomanian/Turonian boundary interval were insufficient or not active to disrupt the terrestrial community or to cause malformation in land plant reproductive structures.

Materials and methods

For the initial palynological study of the Cassis section, a total of 67 rock samples were prepared by the Geological Survey of North Rhine-Westphalia in Krefeld, Germany. To remove carbonate and silica, cleaned, crushed, and weighed samples (20 to 50 g) were subjected to 30% HCl and 38% HF treatments, respectively, according to the standard palynological preparation[65]. Residues were sieved over an 11-μ m mesh and mounted on microscope slides.

After a rigorous palynological screening of the Cassis section, this research aimed to evaluate the occurrence and the abundance of malformed features in spores and pollen grains across the OAE 2. Following the method established by Galasso et al.[6], we attempted to quantitative and qualitative describes morphological traits in sporomorphs and discriminate between alterations caused by preservation and/or those caused by malformation across the Cenomanian/Turonian boundary.

Data availability

All data generated and/or analysed in this study are included in this published article.

Received: 21 November 2022; Accepted: 15 February 2023
Published online: 22 February 2023

References

1. Benca, J. P., Duijnstee, I. A. & Looy, C. V. Fossilized pollen malformations as indicators of past environmental stress and meiotic disruption: Insights from modern conifers. *Paleobiology*, 1–34 (2022).
2. Marshall, J. E., Lakin, J., Troth, I. & Wallace-Johnson, S. M. Uv-b radiation was the devonian-carboniferous boundary terrestrial extinction kill mechanism. *Sci. Adv.* **6**, eaba0768 (2020).
3. Looy, C. V., Twitchett, R. J., Dilcher, D. L., Van Konijnenburg-Van Cittert, J. H. & Visscher, H. Life in the end-permian dead zone. *Proc. Natl. Acad. Sci.* **98**, 7879–7883 (2001).
4. Foster, C. & Afonin, S. Abnormal pollen grains: An outcome of deteriorating atmospheric conditions around the permian-triassic boundary. *J. Geol. Soc.* **162**, 653–659 (2005).
5. Hochuli, P. A., Schneebeli-Hermann, E., Mangerud, G. & Bucher, H. Evidence for atmospheric pollution across the permian-triassic transition. *Geology* **45**, 1123–1126 (2017).
6. Galasso, F., Bucher, H. & Schneebeli-Hermann, E. Mapping monstrosity: Malformed sporomorphs across the smithian/spathian boundary interval and beyond (salt range, pakistan). *Global Planet. Change* **219**, 103975 (2022).
7. Van de Schootbrugge, B. *et al.* Floral changes across the triassic/jurassic boundary linked to flood basalt volcanism. *Nat. Geosci.* **2**, 589–594 (2009).
8. Lindström, S. *et al.* Volcanic mercury and mutagenesis in land plants during the end-triassic mass extinction. *Sci. Adv.* **5**, eaaw4018 (2019).
9. Gravendyck, J., Schobben, M., Bachelier, J. B. & Kürschner, W. M. Macroecological patterns of the terrestrial vegetation history during the end-triassic biotic crisis in the central european basin: A palynological study of the bonenburg section (nw-germany) and its supra-regional implications. *Global Planet. Change* **194**, 103286 (2020).
10. Vilas-Boas, M., Pereira, Z., Cirilli, S., Duarte, L. V. & Fernandes, P. New data on the palynology of the triassic-jurassic boundary of the silves group, lusitanian basin, portugal. *Rev. Palaeobot. Palynol.* **290**, 104426 (2021).

11. Galasso, F., Feist-Burkhardt, S. & Schneebeli-Hermann, E. The palynology of the toarcian oceanic anoxic event at dormettingen, southwest germany, with emphasis on changes in vegetational dynamics. *Rev. Palaeobotany Palynol.* **304**, 104701 (2022).
12. Galasso, F., Feist-Burkhardt, S. & Schneebeli-Hermann, E. Do spores herald the toarcian oceanic anoxic event?. *Rev. Palaeobot. Palynol.* **306**, 104748 (2022).
13. Hay, W. W. & Floegel, S. New thoughts about the cretaceous climate and oceans. *Earth Sci. Rev.* **115**, 262–272 (2012).
14. Faucher, G., Erba, E., Bottini, C. & Gambacorta, G. Calcareous nannoplankton response to the latest cenomanian oceanic anoxic event 2 perturbation. *RIVISTA ITALIANA DI PALEONTOLOGIA E STRATIGRAFIA* (2017).
15. Cohen, K. M., Finney, S. C., Gibbard, P. L. & Fan, J.-X. The ics international chronostratigraphic chart. *Epis. J. Int. Geosci.* **36**, 199–204 (2013).
16. Caron, M. & Homewood, P. Evolution of early planktic foraminifers. *Mar. Micropaleontol.* **7**, 453–462 (1983).
17. Jarvis, I. *et al.* Microfossil assemblages and the cenomanian-turonian (late cretaceous) oceanic anoxic event. *Cretac. Res.* **9**, 3–103 (1988).
18. Huber, B. T., Leckie, R. M., Norris, R. D., Bralower, T. J. & CoBabe, E. Foraminiferal assemblage and stable isotopic change across the cenomanian-turonian boundary in the subtropical north atlantic. *J. Foraminiferal Res.* **29**, 392–417 (1999).
19. Culver, S. J. & Rawson, P. F. *Biotic response to global change: The last 145 million years* (Cambridge University Press, 2006).
20. Erba, E. Calcareous nannofossils and mesozoic oceanic anoxic events. *Mar. Micropaleontol.* **52**, 85–106 (2004).
21. Gebhardt, H., Kuhnt, W. & Holbourn, A. Foraminiferal response to sea level change, organic flux and oxygen deficiency in the cenomanian of the tarfaya basin, southern morocco. *Mar. Micropaleontol.* **53**, 133–157 (2004).
22. Hardenbol, J. *et al.* Mesozoic and cenozoic sequence chronostratigraphic framework of european basins. *Soc. Sediment. Geol.* (1998).
23. Miller, K. G. *et al.* The phanerozoic record of global sea-level change. *Science* **310**, 1293–1298 (2005).
24. Voigt, S., Gale, A. S. & Voigt, T. Sea-level change, carbon cycling and palaeoclimate during the late cenomanian of northwest europe; an integrated palaeoenvironmental analysis. *Cretac. Res.* **27**, 836–858 (2006).
25. Haq, B. U. Cretaceous eustasy revisited. *Global Planet. Change* **113**, 44–58 (2014).
26. Sames, B. *et al.* Short-term sea-level changes in a greenhouse world-a view from the cretaceous. *Palaeogeogr. Palaeoclimatol. Palaeoecol.* **441**, 393–411 (2016).
27. Arthur, M. A., Dean, W. E. & Pratt, L. M. Geochemical and climatic effects of increased marine organic carbon burial at the cenomanian/turonian boundary. *Nature* **335**, 714–717 (1988).
28. Tsikos, H. *et al.* Carbon-isotope stratigraphy recorded by the cenomanian-turonian oceanic anoxic event: Correlation and implications based on three key localities. *J. Geol. Soc.* **161**, 711–719 (2004).
29. Jarvis, I., Lignum, J. S., Gröcke, D. R., Jenkyns, H. C. & Pearce, M. A. Black shale deposition, atmospheric co2 drawdown, and cooling during the cenomanian-turonian oceanic anoxic event. *Paleoceanography***26** (2011).
30. van Bentum, E. C., Reichart, G.-J. & Damsté, J. S. S. Organic matter provenance, palaeoproductivity and bottom water anoxia during the cenomanian/turonian oceanic anoxic event in the newfoundland basin (northern proto north atlantic ocean). *Org. Geochem.* **50**, 11–18 (2012).
31. Owens, J. D., Lyons, T. W. & Lowery, C. M. Quantifying the missing sink for global organic carbon burial during a cretaceous oceanic anoxic event. *Earth Planet. Sci. Lett.* **499**, 83–94 (2018).
32. Bralower, T. J. Calcareous nannofossil biostratigraphy and assemblages of the cenomanian-turonian boundary interval: Implications for the origin and timing of oceanic anoxia. *Paleoceanography* **3**, 275–316 (1988).
33. Leckie, R. M., Bralower, T. J. & Cashman, R. Oceanic anoxic events and plankton evolution: Biotic response to tectonic forcing during the mid-cretaceous. *Paleoceanography* **17**, 13–1 (2002).
34. Slater, S. M., Bown, P., Twitchett, R. J., Danise, S. & Vajda, V. Global record of "ghost" nannofossils reveals plankton resilience to high co2 and warming. *Science* **376**, 853–856 (2022).
35. Forster, A., Schouten, S., Moriya, K., Wilson, P. A. & Sinninghe Damsté, J. S. Tropical warming and intermittent cooling during the cenomanian/turonian oceanic anoxic event 2: Sea surface temperature records from the equatorial atlantic. *Paleoceanography***22** (2007).
36. Barclay, R. S., McElwain, J. C. & Sageman, B. B. Carbon sequestration activated by a volcanic co2 pulse during ocean anoxic event 2. *Nat. Geosci.* **3**, 205–208 (2010).
37. Damsté, J. S. S., van Bentum, E. C., Reichart, G.-J., Pross, J. & Schouten, S. A co2 decrease-driven cooling and increased latitudinal temperature gradient during the mid-cretaceous oceanic anoxic event 2. *Earth Planet. Sci. Lett.* **293**, 97–103 (2010).
38. Heimhofer, U. *et al.* Vegetation response to exceptional global warmth during oceanic anoxic event 2. *Nat. Commun.* **9**, 1–8 (2018).
39. Huber, B. T., MacLeod, K. G., Watkins, D. K. & Coffin, M. F. The rise and fall of the cretaceous hot greenhouse climate. *Global Planet. Change* **167**, 1–23 (2018).
40. Robinson, S. A. *et al.* Southern hemisphere sea-surface temperatures during the cenomanian-turonian: Implications for the termination of oceanic anoxic event 2. *Geology* **47**, 131–134 (2019).
41. Voigt, S., Gale, A. S. & Flögel, S. Midlatitude shelf seas in the cenomanian-turonian greenhouse world: Temperature evolution and north atlantic circulation. *Paleoceanography***19** (2004).
42. Van Helmond, N. *et al.* Freshwater discharge controlled deposition of cenomanian-turonian black shales on the nw european epicontinental shelf (wunstorf, north germany). *Clim. Past Discuss* **10**, 3755–3786 (2014).
43. Li, Y.-X., Montanez, I. P., Liu, Z. & Ma, L. Astronomical constraints on global carbon-cycle perturbation during oceanic anoxic event 2 (oae2). *Earth Planet. Sci. Lett.* **462**, 35–46 (2017).
44. O'Brien, C. L. *et al.* Cretaceous sea-surface temperature evolution: Constraints from tex86 and planktonic foraminiferal oxygen isotopes. *Earth Sci. Rev.* **172**, 224–247 (2017).
45. Jones, C. E. & Jenkyns, H. C. Seawater strontium isotopes, oceanic anoxic events, and seafloor hydrothermal activity in the jurassic and cretaceous. *Am. J. Sci.* **301**, 112–149 (2001).
46. Snow, L. J., Duncan, R. A. & Bralower, T. J. Trace element abundances in the rock canyon anticline, pueblo, colorado, marine sedimentary section and their relationship to caribbean plateau construction and oxygen anoxic event 2. *Paleoceanography***20** (2005).
47. Kuroda, J. *et al.* Contemporaneous massive subaerial volcanism and late cretaceous oceanic anoxic event 2. *Earth Planet. Sci. Lett.* **256**, 211–223 (2007).
48. Turgeon, S. C. & Creaser, R. A. Cretaceous oceanic anoxic event 2 triggered by a massive magmatic episode. *Nature* **454**, 323–326 (2008).
49. Floegel, S. *et al.* Simulating the biogeochemical effects of volcanic co2 degassing on the oxygen-state of the deep ocean during the cenomanian/turonian anoxic event (oae2). *Earth Planet. Sci. Lett.* **305**, 371–384 (2011).
50. Tegner, C. *et al.* Magmatism and eurekan deformation in the high arctic large igneous province: 40ar-39ar age of kap washington group volcanics, north greenland. *Earth Planet. Sci. Lett.* **303**, 203–214 (2011).
51. Du Vivier, A. D. *et al.* Marine 187os/188os isotope stratigraphy reveals the interaction of volcanism and ocean circulation during oceanic anoxic event 2. *Earth Planet. Sci. Lett.* **389**, 23–33 (2014).
52. Du Vivier, A., Selby, D., Condon, D., Takashima, R. & Nishi, H. Pacific 187os/188os isotope chemistry and u-pb geochronology: Synchroneity of global os isotope change across oae 2. *Earth Planet. Sci. Lett.* **428**, 204–216 (2015).
53. Meyers, P. A. Why are the δ13corg values in phanerozoic black shales more negative than in modern marine organic matter?. *Geochem. Geophys. Geosyst.* **15**, 3085–3106 (2014).

54. Jenkyns, H. C., Dickson, A. J., Ruhl, M. & Van den Boorn, S. H. Basalt-seawater interaction, the plenus cold event, enhanced weathering and geochemical change: Deconstructing oceanic anoxic event 2 (cenomanian-turonian, late cretaceous). *Sedimentology* **64**, 16–43 (2017).
55. Scaife, J. *et al.* Sedimentary mercury enrichments as a marker for submarine large igneous province volcanism? evidence from the mid-cenomanian event and oceanic anoxic event 2 (late cretaceous). *Geochem. Geophys. Geosyst.* **18**, 4253–4275 (2017).
56. Schröder-Adams, C. J., Herrle, J. O., Selby, D., Quesnel, A. & Froude, G. Influence of the high arctic igneous province on the cenomanian/turonian boundary interval, sverdrup basin, high canadian arctic. *Earth Planet. Sci. Lett.* **511**, 76–88 (2019).
57. Jolet, P., Philip, J., Thomel, G., Lopez, G. & Tronchetti, G. Nouvelles données biostratigraphiques sur la limite cénomanien-turonien. la coupe de cassis (sud-est de la france): Proposition d'un hypostratotype européen. *Comptes Rendus de l'Académie des Sciences-Series IIA-Earth and Planetary Science***325**, 703–709 (1997).
58. Bown, P. R. & Young, J. *Calcareous nannofossil biostratigraphy* (Springer, 1998).
59. Green, T., Renne, P. R. & Keller, C. B. Continental flood basalts drive phanerozoic extinctions. *Proc. Natl. Acad. Sci.* **119**, e2120441119 (2022).
60. Percival, L. M. *et al.* Does large igneous province volcanism always perturb the mercury cycle? Comparing the records of oceanic anoxic event 2 and the end-cretaceous to other mesozoic events. *Am. J. Sci.* **318**, 799–860 (2018).
61. Salazar, L. *et al.* Diversity patterns of ferns along elevational gradients in andean tropical forests. *Plant Ecol. Divers.* **8**, 13–24 (2015).
62. Mehltreter, K., Walker, L. R. & Sharpe, J. M. *Fern ecology* (Cambridge University Press, 2010).
63. Carvajal-Hernández, C. I., Gómez-Díaz, J. A., Kessler, M. & Krömer, T. Influence of elevation and habitat disturbance on the functional diversity of ferns and lycophytes. *Plant Ecol. Divers.* **11**, 335–347 (2018).
64. Kürschner, W. M., Batenburg, S. J. & Mander, L. Aberrant classopollis pollen reveals evidence for unreduced (2 n) pollen in the conifer family cheirolepidiaceae during the triassic-jurassic transition. *Proc. Royal Soc. B: Biol. Sci.* **280**, 20131708 (2013).
65. Traverse, A. *Paleopalynology* Vol. 28 (Springer Science & Business Media, 2007).
66. Tyson, R. V. Palynofacies investigation of callovian (middle jurassic) sediments from dsdp site 534, blake-bahama basin, western central atlantic. *Mar. Pet. Geol.* **1**, 3–13 (1984).
67. RV, T. Sedimentary organic matter: Organic facies and palynofacieschapman & hall. *London, 615pp* (1995).
68. Vakhrameyev, V. Classopollis pollen as an indicator of jurassic and cretaceous climate. *Int. Geol. Rev.* **24**, 1190–1196 (1982).
69. Vakhrameev, V. Range and palaeoecology of mesozoic conifers, the cheirolepidiaceae. *Paleontol. Zh.* **1**, 19–34 (1970).
70. WATSON, J. Some lower cretaceous conifers of the cheirolepidiaceae from the usa and england. *Palaeontology* **20**, 715–749 (1977).
71. Fonseca, C., Mendonça Filho, J. G., Lézin, C., De Oliveira, A. D. & Duarte, L. V. Organic matter deposition and paleoenvironmental implications across the cenomanian-turonian boundary of the subalpine basin (se france): Local and global controls. *Int. J. Coal Geol.* **218**, 103364 (2020).
72. Benca, J. P., Duijnstee, I. A. & Looy, C. V. Uv-b-induced forest sterility: Implications of ozone shield failure in earth's largest extinction. *Sci. Adv.* **4**, e1700618 (2018).
73. Wilson, L. A study in variation of picea glauca (moench) voss pollen. *Grana* **4**, 380–387 (1963).
74. Lindström, S., McLoughlin, S. & Drinnan, A. N. Intraspecific variation of taeniate bisaccate pollen within permian glossopterid sporangia, from the prince charles mountains, antarctica. *Int. J. Plant Sci.* **158**, 673–684 (1997).
75. Leitch, A. & Leitch, I. Ecological and genetic factors linked to contrasting genome dynamics in seed plants. *New Phytol.* **194**, 629–646 (2012).
76. Coffin, M. F. & Eldholm, O. Large igneous provinces: crustal structure, dimensions, and external consequences. *Rev. Geophys.* **32**, 1–36 (1994).
77. Wignall, P. B. Large igneous provinces and mass extinctions. *Earth Sci. Rev.* **53**, 1–33 (2001).
78. McElwain, J. C., Wade-Murphy, J. & Hesselbo, S. P. Changes in carbon dioxide during an oceanic anoxic event linked to intrusion into gondwana coals. *Nature* **435**, 479–482 (2005).
79. Bond, D. P., Wignall, P. B., Keller, G. & Kerr, A. Large igneous provinces and mass extinctions: An update. *Volcan., Impacts, Mass Extinc.: Causes Effects* **505**, 29–55 (2014).
80. Burgess, S., Bowring, S., Fleming, T. & Elliot, D. High-precision geochronology links the ferrar large igneous province with early-jurassic ocean anoxia and biotic crisis. *Earth Planet. Sci. Lett.* **415**, 90–99 (2015).
81. Burgess, S. D., Muirhead, J. D. & Bowring, S. A. Initial pulse of siberian traps sills as the trigger of the end-permian mass extinction. *Nat. Commun.* **8**, 1–6 (2017).
82. Ernst, R. E. & Youbi, N. How large igneous provinces affect global climate, sometimes cause mass extinctions, and represent natural markers in the geological record. *Palaeogeogr. Palaeoclimatol. Palaeoecol.* **478**, 30–52 (2017).
83. Ruhl, M. *et al.* Reduced plate motion controlled timing of early jurassic karoo-ferrar large igneous province volcanism. *Sci. Adv.* **8**, eabo0866 (2022).
84. Dickens, G. R., Paull, C. K. & Wallace, P. Direct measurement of in situ methane quantities in a large gas-hydrate reservoir. *Nature* **385**, 426–428 (1997).
85. Courtillot, V. E. & Renne, P. R. On the ages of flood basalt events. *C.R. Geosci.* **335**, 113–140 (2003).
86. Rampino, M. R., Rodriguez, S., Baransky, E. & Cai, Y. Global nickel anomaly links siberian traps eruptions and the latest permian mass extinction. *Sci. Rep.* **7**, 1–6 (2017).
87. Clapham, M. E. & Renne, P. R. Flood basalts and mass extinctions. *Annu. Rev. Earth Planet. Sci.* **47**, 275–303 (2019).
88. McElwain, J. C., Popa, M. E., Hesselbo, S. P., Haworth, M. & Surlyk, F. Macroecological responses of terrestrial vegetation to climatic and atmospheric change across the triassic/jurassic boundary in east greenland. *Paleobiology* **33**, 547–573 (2007).
89. Van de Schootbrugge, B. *et al.* End-triassic calcification crisis and blooms of organic-walled 'disaster species'. *Palaeogeogr. Palaeoclimatol. Palaeoecol.* **244**, 126–141 (2007).
90. Ruckwied, K., Götz, A. E., Pálfy, J. & Török, Á. Palynology of a terrestrial coal-bearing series across the triassic/jurassic boundary (mecsek mts, hungary). *Central Euro. Geol.* **51**, 1–15 (2008).
91. Götz, A., Ruckwied, K., Pálfy, J. & Haas, J. Palynological evidence of synchronous changes within the terrestrial and marine realm at the triassic/jurassic boundary (csővár section, hungary). *Rev. Palaeobot. Palynol.* **156**, 401–409 (2009).
92. Hochuli, P. A., Hermann, E., Vigran, J. O., Bucher, H. & Weissert, H. Rapid demise and recovery of plant ecosystems across the end-permian extinction event. *Global Planet. Change* **74**, 144–155 (2010).
93. Bonis, N. *et al.Palaeoenvironmental changes and vegetation history during the Triassic-Jurassic transition* (LPP Contribution Series No. 29, 2010).
94. Bonis, N. R. & Kürschner, W. M. Vegetation history, diversity patterns, and climate change across the triassic/jurassic boundary. *Paleobiology* **38**, 240–264 (2012).
95. Visscher, H. *et al.* Environmental mutagenesis during the end-permian ecological crisis. *Proc. Natl. Acad. Sci.* **101**, 12952–12956 (2004).

Acknowledgements

We would like to thank the Editorial Board Member Michal Zaton, Evelyn Kustatscher and the other anonymous reviewer for their time in evaluating the manuscript and for their informed comments and remarks. This work

was supported by the Swiss National Science Foundation (project n° 200021_175540/1 to Elke Schneebeli-Hermann). .

Author contributions

U.H. provided the samples and strew mounts. F.G. and E.S.H. conceptualised the study. F.G. analysed and interpreted the results. All authors contributed to the manuscript and approved the final version.

Competing interests

The authors declare no competing interests.

Additional information

Correspondence and requests for materials should be addressed to F.G.

Reprints and permissions information is available at www.nature.com/reprints.

Publisher's note Springer Nature remains neutral with regard to jurisdictional claims in published maps and institutional affiliations.